Thermal degradation of alkyl triphenyl phosphonium intercalated montmorillonites

An isothermal kinetic study

**Saheli Ganguly · Kausik Dana ·
Tapas Kumar Mukhopadhyay ·
Sankar Ghatak**

Abstract The decomposition mechanism of intercalated montmorillonites at a particular temperature region and the activation energy involved in it are the two important aspects which determines the thermal stability of intercalated montmorillonites. In this study, montmorillonite was intercalated with alkyl (methyl, ethyl, propyl, and dodecyl) triphenyl phosphonium intercalates. Differential thermogravimetric analysis of each intercalated montmorillonites showed different peaks with associated organic loss at different temperature zone. Intercalated montmorillonites were subjected to isothermal kinetic analysis corresponding to selected temperature zone obtained from DTG peaks. Activation energies of organic decomposition process at selected temperature zones were determined. Mass spectral analysis and FTIR were done to understand the decomposition mechanisms and to relate them with the estimated activation energies.

Keywords Intercalated montmorillonite · Alkyl triphenyl phosphonium salts · Isothermal kinetic analysis · Decomposition mechanism · Activation energy · Mass spectrometry

Introduction

Surface modifications of clay minerals have received attention because it allows the creation of new materials and new applications. During the last decade, organically

S. Ganguly · K. Dana (✉) · T. K. Mukhopadhyay · S. Ghatak
Advanced Clay and Traditional Ceramics Division, Central
Glass and Ceramic Research Institute, CSIR, 196, Raja S.C.
Mullick Road, Kolkata, West Bengal 700032, India
e-mail: kdana@cgcri.res.in

modified layered silicates (OLSs) have received much attention from scientific and technological communities for its use as nanofillers in polymer clay nanocomposite. The automotive, aerospace, and packaging industries view polymer–clay nanocomposites as promising materials for the twenty-first century due to improved mechanical, thermal, barrier, and flame-retardant properties [1–5]. Apart from polymer clay nanocomposite applications, these intercalated montmorillonites are also being used as rheological modifier, adsorbents of pollutants in waste water treatments, thickening and gelling agents in paints and lubricants, as drug delivery vehicle in medicinal field etc. [6, 7]. Modification of clay minerals with organic materials is necessary to establish compatibility between clay particles and polymer matrix. Montmorillonite is the best-known member of smectite group of clay mineral for intercalation with organics because of its exceptional properties such as high cation exchange capacity, swelling behavior, high adsorption capacity, and large surface area. Montmorillonite unit cell consists of one octahedral Al^{+3}/Mg^{+2} sheet sandwiched between two tetrahedral Si^{+4} sheet with variable isomorphic octahedral lattice substitution (Al^{+3} substituted by Mg^{+2}). This results in charge imbalance in the lattice which is neutralized by adsorption of inorganic cations. Stacking of the unit layers occur along c axis [8–10]. Organic cations can be intercalated within interlayer space of montmorillonite through ion exchange with interlayer inorganic cations, often called exchangeable cations. Considerable studies have been done using different intercalates with varying chain length and their relative proportion [11–27]. Relation between structures of organic intercalates and stability of the intercalated montmorillonites is of paramount importance in the context of clay–polymer nanocomposites. A more detailed knowledge of organic decomposition processes of intercalated

montmorillonites during heat treatment is needed to make further progress in the field of structure and stability of these modified clay minerals. There have been fewer attempts to probe thoroughly the kinetics of dehydration of montmorillonites. Girgis et al. [28] conducted non-isothermal kinetic study on a series of Ca-smectites and concluded that dehydration followed a first-order reaction with activation energy values ranging from 39.8 to 52.3 kJ mol^{-1}. Furthermore, Guler and Sarier [29] arrived at a value of 14.72 kJ mol^{-1} for a similar type of experimental set up following the work of Murray and White. However, it should be noted that Murray and White [30–35] studied dehydroxylation of clay minerals. Onal and Sarikaya [15] have studied the kinetics of decomposition of some ammonium modified smectite following nonisothermal method using Coats and Red fern equation. The decomposition was assumed to be first-order reaction such as, solid (1) → solid (2) + gas. However, isothermal kinetic analyses of intercalated montmorillonite decomposition processes have not been studied so far. The principle objective of this study is to determine the effect of temperature on the rate of organic decomposition reaction. Comparative analysis of kinetic rate constants, activation energies of organic decomposition process with different intercalate structures enable inferences to be made concerning the reaction mechanisms or to get an idea about the sequence of chemical steps at particular temperatures.

Experimental

Materials

Montmorillonites, M (PGV, Nanocor, USA) was used as received in this study. M was converted to Na$^+$ form by ion exchange. CEC of M was determined by titration with EDTA-complexometric method [36, 37] and was found to be 88 Cmol kg^{-1} of clay. The triphenyl phosphonium intercalates used in this study were marked as Ph$_3$C$_1$, Ph$_3$C$_2$, Ph$_3$C$_3$, Ph$_3$C$_{12}$ where the alkyl group was varied as CH$_3$, C$_2$H$_5$, C$_3$H$_7$ and C$_{12}$H$_{25}$ (Fig. 1). These were supplied by Sigma-Aldrich.

Sample preparation

Intercalation of M with alkyl triphenyl phosphonium salts: 1 g clay was dispersed in 250 mL deionized water and ultrasonicated (0.5 W cm^{-2}) for 60 min at temperature ∼70–80 °C. Then, the suspension was stirred on a hot plate set at ∼70–80 °C. 200 mL intercalate solution (M/100) was added drop wise into this suspension. After
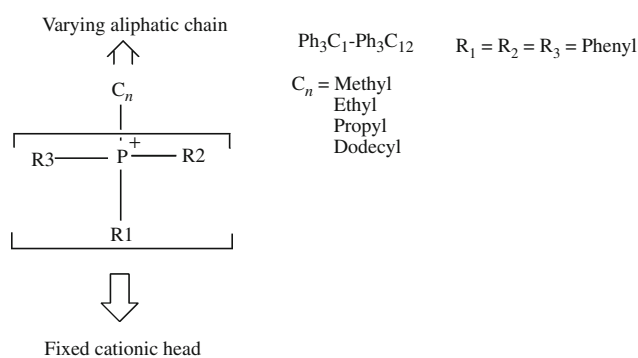
Fig. 1 Structure of intercalates

addition of intercalate, it was kept under constant stirring at ∼70–80 °C for 1 h. The reaction mixture was kept overnight for settling. The supernatant water with excess surfactant was decanted, and the flock was redispersed in water. The process was repeated for three times. Then, it was filtered under suction and washed with 2,000 mL hot water. The collected product was dried at 70 °C in vacuum drier for ∼24 h. The dried product was ground in an agate mortar pestle and kept in sealed glass bottles. Before kinetic analysis, the intercalated samples were heated up to 200 °C to remove adsorbed and interlayer water.

Characterization

X-ray diffraction (XRD)

The studies on basal spacing of montmorillonite and intercalated montmorillonite were done in XPERT-PRO (PANALYTICAL) diffractometer system. The system was operated at 30 mA, 40 kV between 2.0 and 10.0 (2θ) at a step of 0.05.

Thermogravimetry (TG)

TG analysis of the samples was carried out using instrument Model OKAY, Bysakh and Co., India. The system was operated at a heating rate 10 °C min^{-1} from 30 to 800 °C in ambient atmosphere with ∼50 mg sample in alumina crucible.

Mass spectroscopy

Intercalated clay samples were dissolved in organic solvent. The organic layer was decanted and evaporated. Then, the sample was analyzed by mass spectroscopy with Qtof Micro YA263 (TOF MS ES+) instrument.
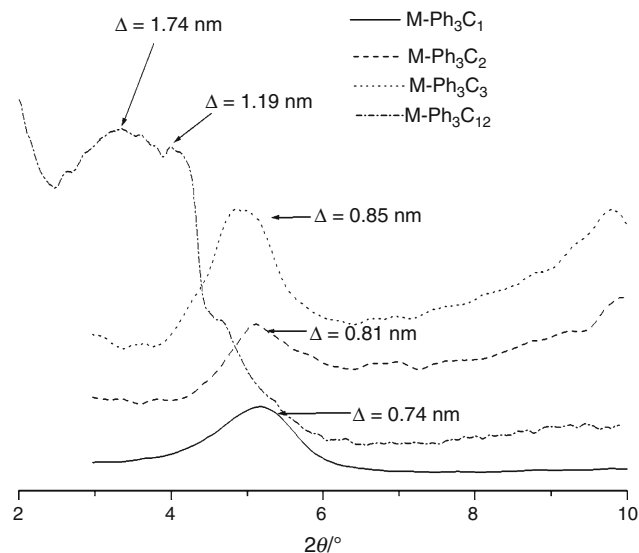
Fourier transform infra-red spectroscopy

Fourier transform infra-red spectra (FTIR) have been recorded with the Nicolet 5700, Thermo Electron Corporation, using KBr pellet.

Result and discussion

XRD analysis

Intercalation of montmorillonites was evidenced by XRD analysis. Experimental montmorillonites showed basal spacing (d_{001}) ∼ 1.25 nm, which corresponds to sodium-montmorillonite (5,9). The smectite group of minerals shows variable integral series of basal spacing (d_{001}) which is dependent upon the size of exchangeable cation and on the degree of hydration of the cation (8). XRD plots of intercalated montmorillonite (Fig. 2) showed that intercalation by ion exchange with the phosphonium intercalates increased basal spacing (d_{001}) of experimental montmorillonite due to removal of smaller interlayer Na$^+$ by larger phosphonium ions. The gallery height (Δ = corresponds to the thickness of organo cation layer sandwiched between two clay mineral layers) was calculated by subtracting the standard average thickness of one montmorillonites layer (0.96 nm) from the observed d_{001} (8.9). The plot showed diffused and multiple peaks in M-Ph₃C₁₂ (Fig. 2) which established coexistence of different interlayers. Superposition of reflections corresponding to these different interlayers distances created the wide, diffused and multiple peaks implying co-existence of different intergallery arrangements of intercalates.

TG analysis

Isothermal kinetic studies

To understand about the nature of bonding in the prepared intercalated montmorillonites, a detailed analysis was undertaken through isothermal thermogravimetric analysis. The weight loss of the samples followed exponential relationship (Fig. 3) with time which suggests the application of first-order kinetics. The reaction which takes place during heating of intercalated montmorillonites is solid (1) → solid (2) + gas. If the weight and the volume of the initial sample are kept fixed, the concentration may be replaced by weight loss. Thus, at a given temperature if L is the weight loss of the sample at time t and L_{inf} is the total weight loss at infinite time, then L_{inf} is equivalent to the initial concentration of organics to be decomposed at that particular experimental temperature as each sample was preheated at 200 °C to remove adsorbed water. Therefore, $L_{inf} - L$ is equivalent to the concentration of organics remaining in the sample at time t. Therefore, according to the first-order kinetics the rate of loss of organics will be given by the Eq. 1.

$$dL/dt = -k(L_{inf} - L). \tag{1}$$

$$\log_{10}\{(L_{inf} - L)/L_{inf}\} = -kt/2.303. \tag{2}$$

Equation 1 permits the evaluation of rate constants (k) for organic decomposition process from the slope of the straight line obtained by plotting $\log_{10}(L_{inf} - L)/L_{inf}$ versus t provided we know the value of L_{inf}. L_{inf} was determined from the weight loss after heating the sample at the particular experimental temperature till constant weight persists. ln k can be plotted against $1/T$ to calculate the

Fig. 2 XRD plots of M-Ph₃C₁–M-Ph₃C₁₂
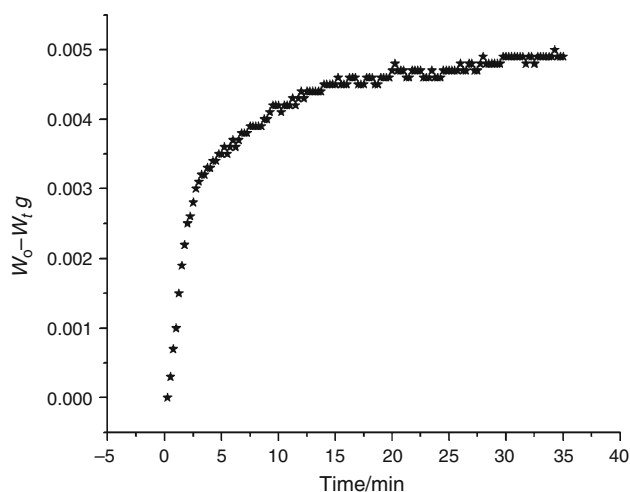
Fig. 3 Time versus mass loss curve for M-Ph₃C₁ at 295 °C
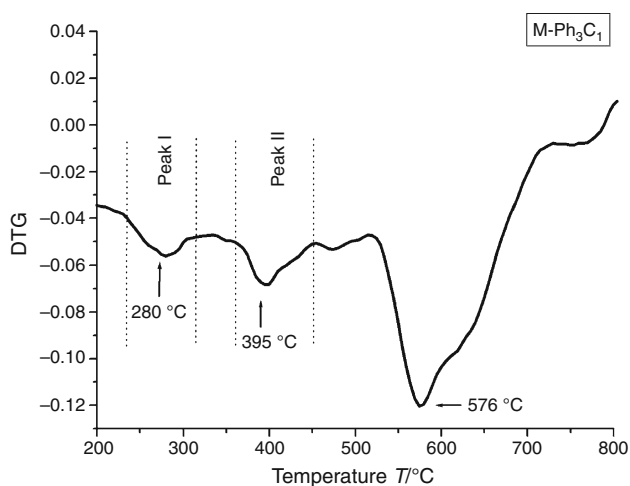
Fig. 4 DTG curve of M-Ph$_3$C$_1$

activation energy of organic decomposition process following the Arrhenius equation.

$$\ln k = \ln A - E/8.314T \qquad (3)$$

where E is the activation energy, A is the preexponential factor, T is the temperature in K.

Mass loss zones In this study, montmorillonites were intercalated with alkyl triphenyl phosphonium intercalates varying the alkyl chain length (methyl, ethyl, propyl, and dodecyl). Each intercalated montmorillonites were subjected to thermo gravimetric analysis. The differential thermogravimetric (DTG) curves showed organic loss and structural water loss which gave rise of multiple peaks in different temperature regions (Fig. 4). As organic decomposition of intercalated montmorillonites took place above 250 °C [11, 13], DTG peaks above 250 °C were only considered for kinetic analysis. DTG peaks above 550 °C were also excluded from present kinetic analysis due to the fact that this is an overlapping region of organic loss and structural water loss. The temperature zone of each DTG peak of intercalated montmorillonites was selected as given in corresponding DTG plots (Fig. 4). Methyl triphenyl phosphonium (M-Ph$_3$C$_1$) intercalated montmorillonite showed two organic mass loss peak within 250–550 °C temperature region, one was in lower temperature and the other was at higher temperature region (Fig. 4). Temperature zone associated with each peak was selected and is furnished in Table 1. Peak I temperature region designated the temperature zone of lower temperature peak and peak II temperature region signified the higher one. Similarly, ethyl and propyl triphenyl phosphonium intercalated montmorillonites (M-Ph$_3$C$_2$ and M-Ph$_3$C$_3$) showed three organic mass loss peaks within above said temperature
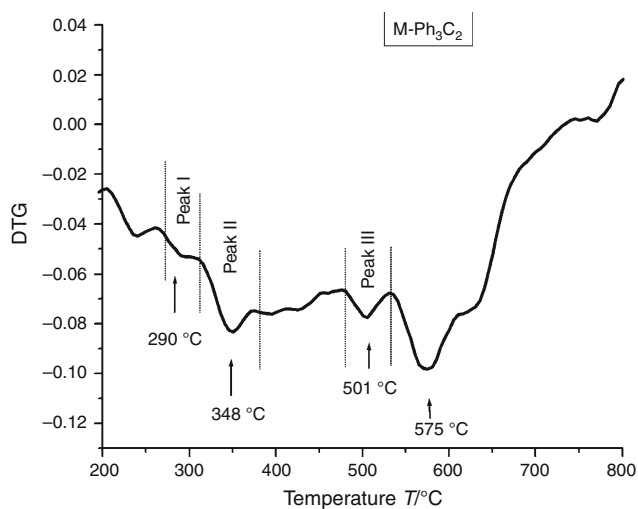
region (Figs. 5, 6) and corresponding temperature region was designated as peak I, peak II, and peak III (Table 1). However, dodecyl triphenyl phosphonium intercalated montmorillonites (M-Ph$_3$C$_{12}$) showed a single peak only in lower temperature region (Fig. 7)

Rate constant and validity of 1st order kinetics However, all the intercalated montmorillonites were heated at different temperatures within the selected temperature zones, and time versus mass loss measurements were done at those temperatures. Plot of $\log_{10}\{(L_{inf} - L)/L_{inf}\}$ versus t was found to be a straight line where two slopes coincide (Fig. 8). One representative plot of M-Ph$_3$C$_1$ heated at 295 °C is furnished to demonstrate the slopes which constituted the line. Two slopes indicated that two reaction rates were involved in organic decomposition. This again implied that different reaction pathways were operating during decomposition process. Consequently, for each $\log_{10}\{(L_{inf} - L)/L_{inf}\}$ versus t plot, two rate constants k_1 and k_2 were deduced. As the plots provided two slopes, fraction of mass loss associated with each slope was also evaluated. The rate constants (k_1, k_2) and percent decomposition of the total loss (W) associated with the first slope are furnished in Table 1. Percent decomposition of the total loss (W) associated with the first slope indicated the extent up to which the first-reaction rate (k_1) was continued during the organic decomposition. It was observed that for a particular intercalated montmorillonite, the percent decomposition of the total loss (W) related with the first slope gradually diminished at higher temperature peaks. For example, in M-Ph$_3$C$_1$, 49–89% of the total loss was associated with the first slope in peak I temperature region which decreased in peak II temperature region to 38–53%. Similarly, in M-Ph$_3$C$_2$, 51–92% of the total loss was associated with the first slope in peak I region which decreased to 36–65% in peak II and 38–47% in peak III temperature region. Similar trend was followed by M-Ph$_3$C$_3$. M-Ph$_3$C$_{12}$ gave only one peak, and percent decomposition of the total loss for the first slope was 19–39% (Table 1).
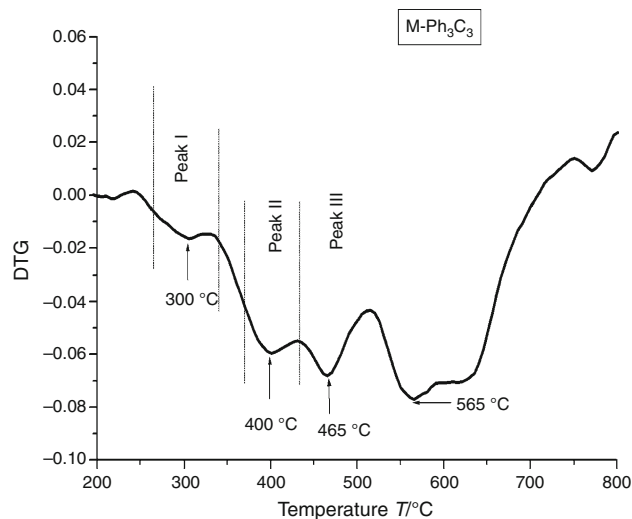
Activation energy The ln k versus 1/T graphs for organic decomposition process of intercalated montmorillonites with different alkyl triphenyl phosphonium salts were plotted (Figs. 9, 10, 11, 12, 13, 14, 15, 16). The activation energy values deduced from the slope of the above plots are presented in Table 2. As heat treatment of intercalated montmorillonites in peak I, peak II, and/or peak III peak temperature regions provided two reaction rates (Table 1), it gave rise of two different activation energy values (Table 2). The observations implied that the decomposition of organics within intercalated montmorillonites involved

**Table 1** List of different rate constants at different temperatures

Intercalated clay	Peak I temperature zone				Peak II temperature zone				Peak III temperature zone			
	$T/°C$	k_1/min^{-1}	$W/\%$	k_2/min^{-1}	$T/°C$	k_1/min^{-1}	$W/\%$	k_2/min^{-1}	$T/°C$	k_1/min^{-1}	$W/\%$	k_2/min^{-1}
M-Ph$_3$C$_1$	250	0.373	89	0.090	355	0.228	53	0.090				
	265	0.338	68	0.067	370	0.217	48	0.078				
	280	0.313	69	0.082	385	0.238	45	0.109				
	295	0.367	49	0.086	400	0.204	47	0.204				
	310	0.471	55	0.107	415	0.317	38	0.317				
					430	0.202	50	0.202				
M-Ph$_3$C$_2$	250	0.359	92	0.104	325	0.209	48	0.069	460	0.081	41	0.116
	265	0.328	56	0.114	340	0.390	65	0.108	475	0.091	47	0.087
	280	0.391	74	0.391	355	0.246	36	0.067	490	0.102	43	0.147
	295	0.297	51	0.297	370	0.247	50	0.095	505	0.101	46	0.113
	310	0.438	57	0.175					520	0.087	40	0.136
									535	0.093	38	0.143
M-Ph$_3$C$_3$	250	0.295	86	0.095	355	0.188	39	0.070	445	0.078	41	0.119
	265	0.237	53	0.067	370	0.174	40	0.070	460	0.080	42	0.142
	280	0.394	69	0.094	385	0.163	31	0.067	475	0.084	33	0.143
	295	0.341	57	0.100	400	0.201	30	0.073	490	0.089	39	0.147
	310	0.288	61	0.112	415	0.154	31	0.087	505	0.081	30	0.148
					430	0.204	31	0.099	520	0.087	35	0.170
M-Ph$_3$C$_{12}$	265	0.119	39	0.039								
	280	0.108	35	0.037								
	295	0.118	17	0.038								
	310	0.183	25	0.057								
	325	0.135	17	0.047								
	340	0.121	23	0.058								
	355	0.124	19	0.047								

Fig. 5 DTG curve of M-Ph$_3$C$_2$
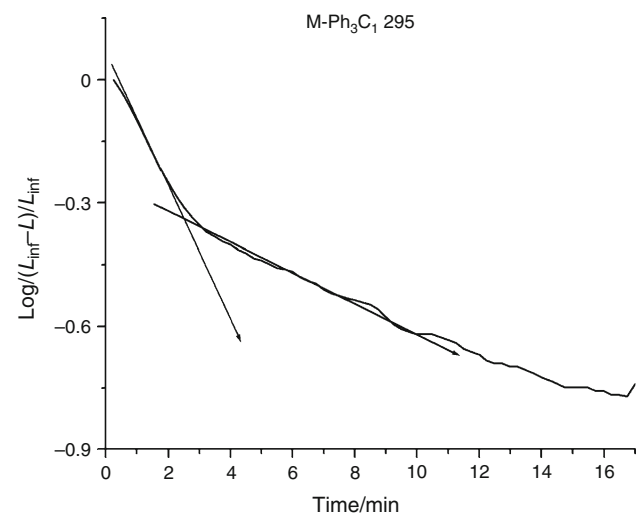

Fig. 6 DTG curve of M-Ph$_3$C$_3$

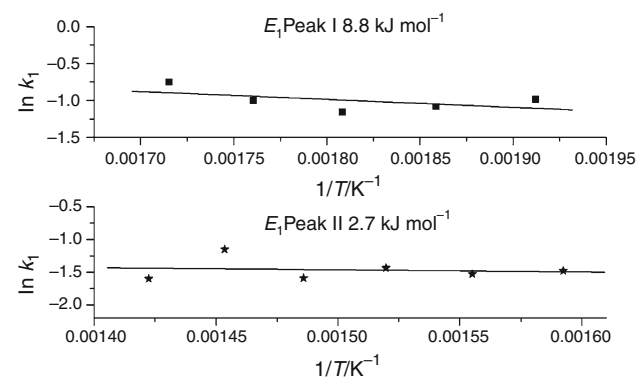breaking of anchorages of different energies. During heat treatment, several bonds of organic intercalates were broken, and different fragments and compounds were produced in different decomposition pathways. The activation energy values included contributions from those decomposition pathways.
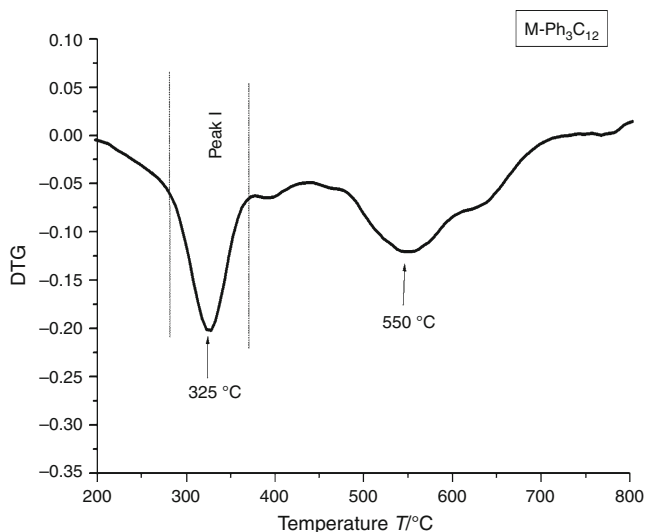
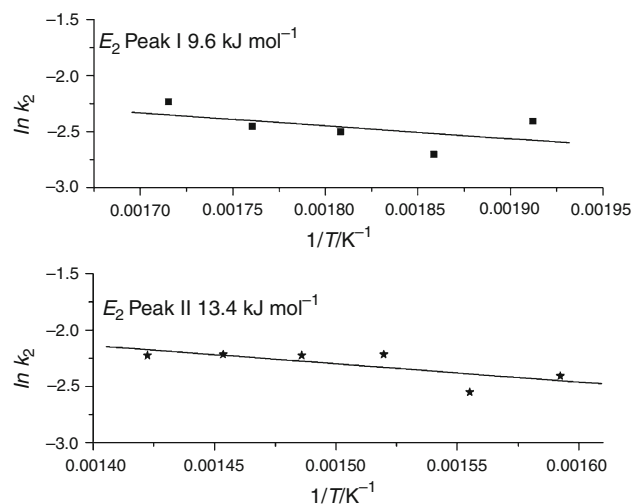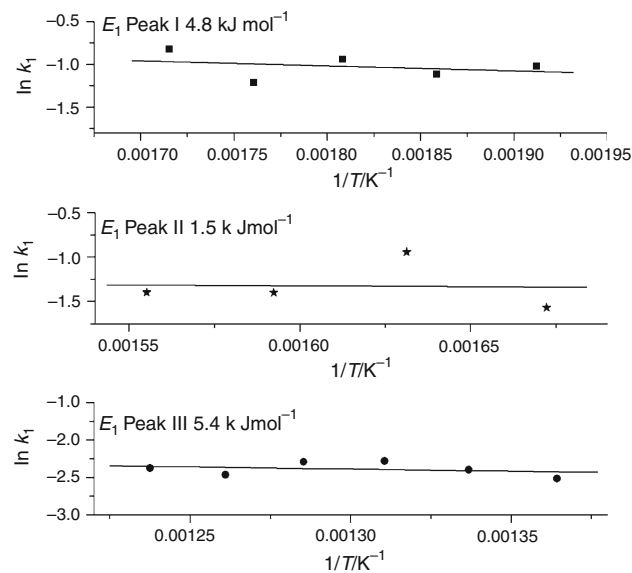Fig. 7 DTG curve of M-Ph$_3$C$_{12}$

Fig. 10 Activation energy plot (E_2) for peak I and peak II of M-Ph$_3$C$_1$

Fig. 8 Time versus Log($\{L_{inf} - L\}/L_{inf}$) plot of M-Ph$_3$C$_1$ at 295 °C

Fig. 11 Activation energy plot (E_1) for peak I, peak II, and peak III of M-Ph$_3$C$_2$

Possible mechanisms To explain the type of major reaction pathways that occurred during decomposition, mass spectral analysis of M-Ph$_3$C$_3$ was done. M-Ph$_3$C$_3$ were heated at three maximum peak decomposition temperature of peak I, peak II, and peak III (300, 400, and 465 °C), and the heat treated sample was subjected to mass spectral analysis to analyze the residual fragment after heating the compound at that temperature. The major mass spectra peak of M-Ph$_3$C$_3$ heated at 300 °C, i.e., at the maximum peak decomposition temperature of peak I, was at the *m/z* value of 305 and 279 (Fig. 17). 305 *m/z* was the molecular weight of undecomposed propyl triphenyl
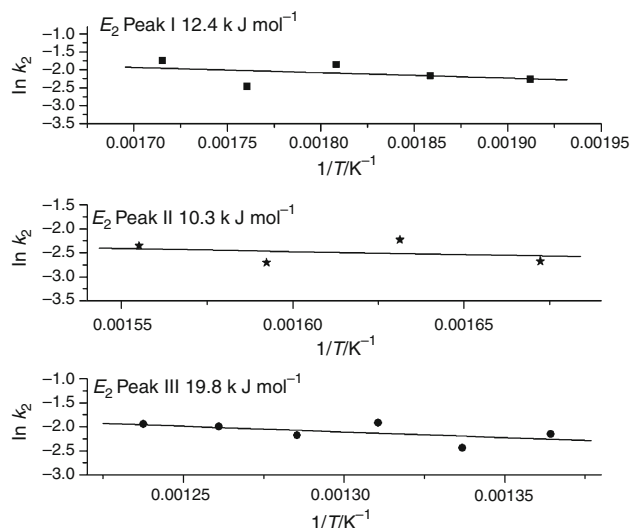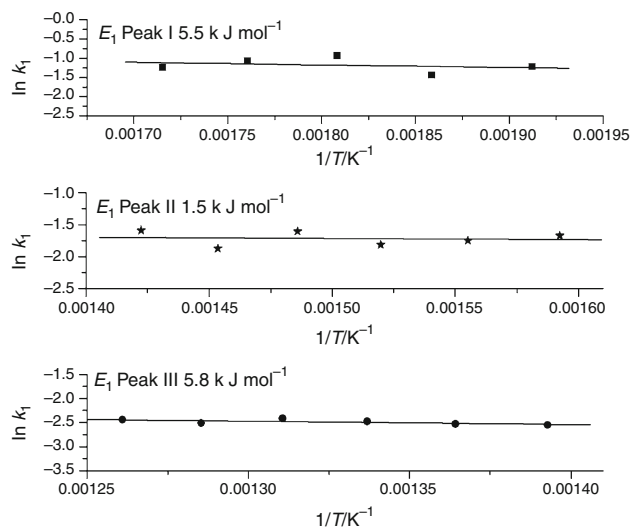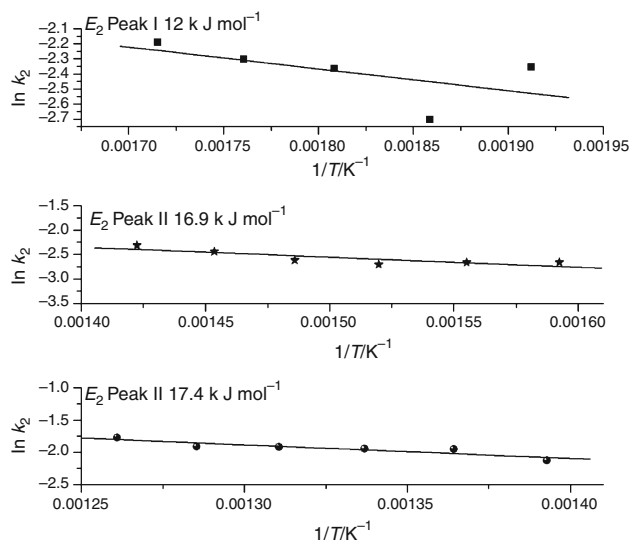

Fig. 9 Activation energy plot (E_1) for peak I and peak II of M-Ph$_3$C$_1$

Fig. 12 Activation energy plot (E_2) for peak I, peak II, and peak III of M-Ph$_3$C$_2$

Fig. 13 Activation energy plot (E_1) for peak I, peak II, and peak III of M-Ph$_3$C$_3$

Fig. 14 Activation energy plot (E_2) for peak I, peak II, and peak III of M-Ph$_3$C$_3$

Fig. 15 Activation energy plot (E_1) for peak I of M-Ph$_3$C$_{12}$

phosphonium cation and 279 m/z closely matched with the molecular weight of triphenyl phosphine oxide (277). The presence of these fragments revealed that major part of propyl triphenyl phosphonium salt intercalated montmorillonite, when heated within the temperature region of 250–310 °C, remained undecomposed. A small part of inserted organics within interlayer space of montmorillonites decomposed to yield triphenyl phosphine oxide at the above said temperature region. According to Xie et al. [13], decomposition of alkyl triphenyl phosphonium intercalated montmorillonites gave triphenyl phosphine oxide during heating in the presence of nucleophile OH$^-$. It was observed in previous experiments that in spite of the

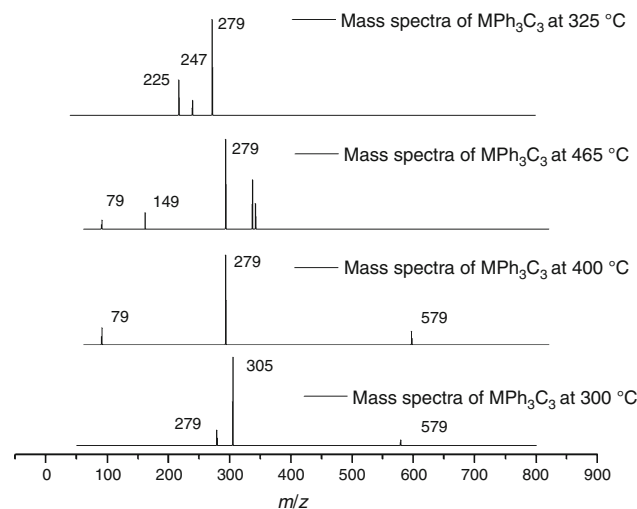preheating of intercalated montmorillonites at 200 °C, little moisture resorption took place [16]. Besides, during decomposition all intercalated montmorillonites were heated in ambient atmosphere. Therefore, nucleophilic attack at phosphonium cation was quite possible. Due to nucleophilic attack at phosphorous, alkyl group was expelled and rearrangement within the residual species led to the formation of triphenyl phosphine oxide (Scheme 1). As stated in our earlier article [16], during intercalation within montmorillonites, adsorption of organic cations occurred at clay mineral surface. These excess adsorbed cations were mainly attached by Van der Waals forces. The intercalated cations were more strongly confined within the interlayer space. However, the surface adsorbed molecules were less strongly attached with the clay surfaces. The
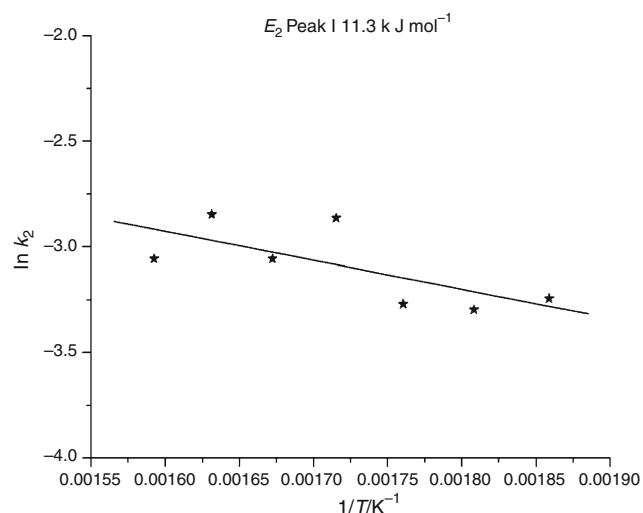
Fig. 16 Activation energy plot (E_2) for peak I of M-Ph$_3$C$_{12}$

Fig. 17 Mass spectra of selected samples

mass spectral data pointed toward the fact that surface adsorbed propyl triphenyl phosphonium cations desorbed and decomposed when heated at temperatures corresponding to peak I region but strongly bonded intercalated part of the cations remained thermally stable during the heat treatment.

Activation energies for different processes Thermal treatment of each intercalated montmorillonites within peak I temperature zone gave two activation energies which was assigned to two types of reactions involved. Surface adsorbed organic cations were of two kinds. Primary organic molecular layers, which were directly attached to the clay surface and molecular layers attached with the primary layers mainly by Van der Waals attractions. These primary molecular layers were more strongly held by electrostatic forces rather than the secondary layers. As lower activation energies should be required to overcome Van der Waals attachment, E_1 was assigned to the desorption and decomposition of those secondary layers which were mainly held by Van der Waals attraction. Consequently, E_2 was assigned to the removal of surface attached primary molecular layers. M-Ph$_3$C$_{12}$ gave only one major DTG peak in lower temperature region.

M-Ph$_3$C$_{12}$ was pretreated similarly as M-Ph$_3$C$_3$ for mass spectral analysis to realize the decomposition pattern of it. So, mass analysis of M-Ph$_3$C$_{12}$ was done after heating it at 325 °C, i.e., the maximum peak decomposition temperature of peak I of the sample. The mass spectra plot has been furnished in Fig. 16. Mass spectral result of M-Ph$_3$C$_{12}$ showed major peak at 279 *m/z* with a few minor peaks. This was evident from the result that all the intercalated and surface adsorbed dodecyl triphenyl phosphonium cation decomposed at 265–355 °C temperature region and the major reaction pathway followed by M-Ph$_3$C$_{12}$ was the rearrangement of dodecyl triphenyl phosphonium to triphenyl phosphine oxide. So, the thermal decomposition pattern and stability of intercalated M-Ph$_3$C$_{12}$ were different from that of M-Ph$_3$C$_3$. It can be concluded from above observation that the decomposition pathway was mainly guided by the heating temperature as well as the nature of cationic head group and chain length of intercalate. It was evident from mass spectra analysis of M-Ph$_3$C$_3$ that along with triphenyl phosphine oxide, other minor fragments were formed during decomposition of organics at the temperature region of peak I. The fragment, which gave peak at 579 *m/z*, may be a dimer formed due to any

Table 2 List of activation energies of different intercalated montmorillonites

| Intercalated clay	Peak I temperature zone			Peak II temperature zone			Peak III temperature zone		
	E_1/kJ mol^{-1}	E_2/kJ mol^{-1}	T_{max}/°C	E_1/kJ mol^{-1}	E_2/kJ mol^{-1}	T_{max}/°C	E_1/kJ mol^{-1}	E_2/kJ mol^{-1}	T_{max}/°C
M-Ph$_3$C$_1$	8.8	9.6	280	2.7	13.4	395			
M-Ph$_3$C$_2$	4.8	12.4	290	1.5	10.3	348	5.4	19.8	500
M-Ph$_3$C$_3$	5.5	12.0	300	1.5	16.9	400	5.8	17.4	465
M-Ph$_3$C$_{12}$	3.5	11.3	325						

T_{max} maximum peak decomposition temperature

Scheme 1 Probable reaction path to yield triphenyl phosphine oxide
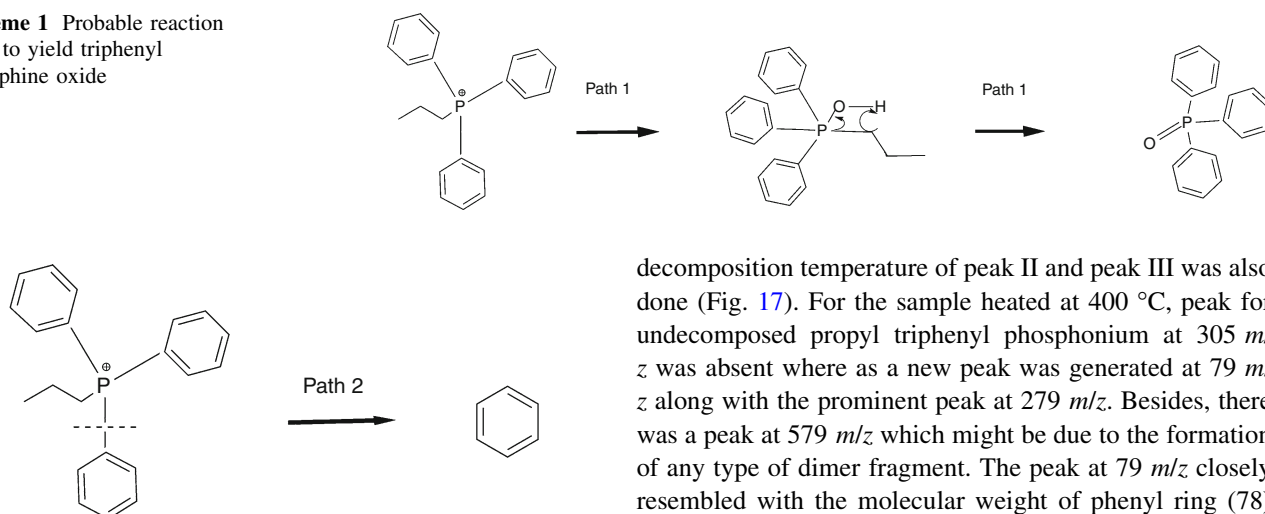
Scheme 2 Cleavage of sp² carbon–phosphorous bond

dimerization reaction at any step of fragmentation. So during low temperature mass loss, alongwith desorption and decomposition, dimerization might have occurred. Activation energies E_1 and E_2, which were derived by heating the intercalated montmorillonites in peak I temperature region, included contributions from all these possible processes. E_1 and E_2 were plotted against chain length of intercalates. The plot of chain length versus E_1 peak I gave a straight line with a negative slope and that of chain length versus E_2 peak I gave a straight line with a positive slope (Figs. 18, 19). The plots revealed that activation energy E_1 of peak I was decreased with increment of carbon in organic chain whereas activation E_2 of peak I followed the reverse trend. Mass analysis of M-Ph$_3$C$_3$ heated at 400 and 465 °C, i.e., maximum peak

decomposition temperature of peak II and peak III was also done (Fig. 17). For the sample heated at 400 °C, peak for undecomposed propyl triphenyl phosphonium at 305 m/z was absent where as a new peak was generated at 79 m/z along with the prominent peak at 279 m/z. Besides, there was a peak at 579 m/z which might be due to the formation of any type of dimer fragment. The peak at 79 m/z closely resembled with the molecular weight of phenyl ring (78) which was also possible to form during the course of reaction at high temperature. The mass spectral data disclosed the fact that when the intercalated montmorillonites were heated at temperatures 250–310 °C of peak I temperature region, intercalated molecules remained stable but beyond this region the entire organic molecules within montmorillonites were decomposed as indicated by the absence of 305 m/z peak from mass spectra analysis. The rearrangement reaction was present at higher temperature region as peak at 279 m/z was present in all the three mass spectral results. The additional species present during heating the intercalated montmorillonites at peak II and III temperature region was the phenyl fragment. All the intercalated molecules were decomposed after two major reaction pathways during higher temperature decomposition. In one reaction path, nucleophilic attack and sequentially rearrangement took place to form triphenyl phosphine oxide (Scheme 1). The other reaction route was
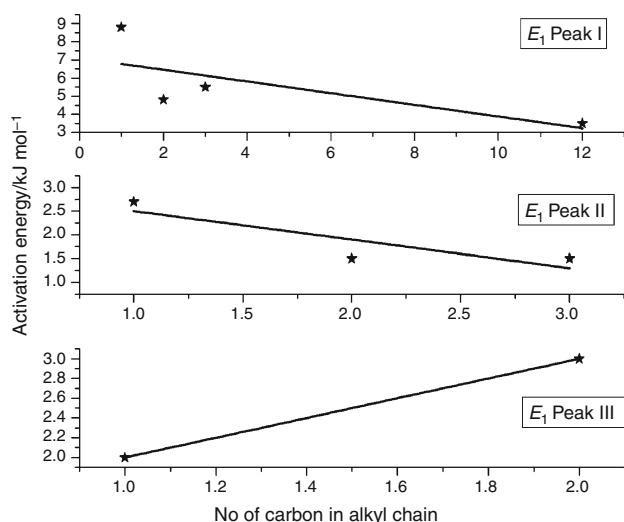
Fig. 18 Plots of chain length versus E_1 of peak I, peak II, and peak III
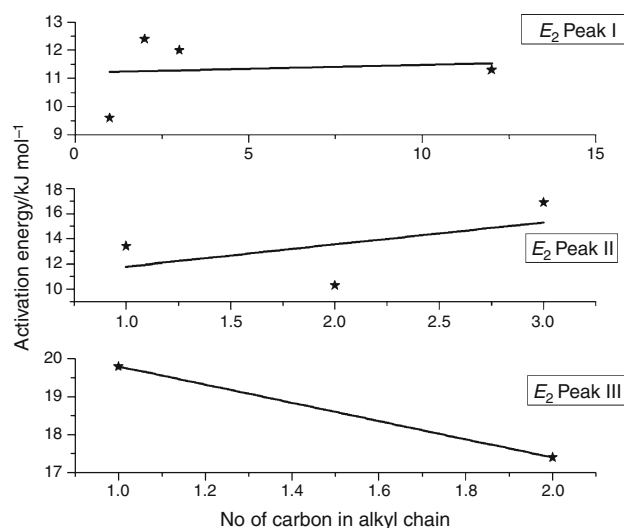
Fig. 19 Plots of chain length versus E_2 of peak I, peak II, and peak III

proceeding through the cleavage of P-sp^2 hybridized carbon bond of phenyl carbon (Scheme 2) leading to the formation of benzene. It was very difficult to assign activation energies E_1 and E_2 deduced from peak II temperature region to each of the above said reaction paths. However, the results from mass spectral analysis revealed that peak 79 m/z was found during higher temperature organic decomposition. So, it was evident that the cleavage of P-phenyl carbon bond initiated at higher temperature which again proved that higher energy was required for that reaction. So, it was quite reasonable to assign that above said reaction process contributed most toward higher activation energy value (E_2). Mass spectral analysis at maximum peak III temperature of M-Ph$_3$C$_3$ (465 °C) showed minor peaks along with the previously recognized peaks at 279 and 79 m/z value. During the heat treatment at 465 °C, decomposition as well as fragmentation occurred at different mechanistic pathways. All these decomposition pathways contributed toward the activation energy values. However, major reaction pathways were same as that heated at 400 °C. The variation of E_1 and E_2 deduced from peak II and peak III temperature zone with chain length of intercalates followed different trends in two different peak regions, respectively (Figs. 18, 19). However, there was a strong correlation of maximum peak decomposition temperature of peak II and peak III with E_2 values of those peaks. For higher maximum peak decomposition temperature, higher E_2 values were found (Table 2). It was observed that E_2 peak II value of M-Ph$_3$C$_1$ was 13.4 kJ mol^{-1}, and its maximum peak decomposition temperature was 395 °C but this value decreased to 10.3 kJ mol^{-1} for M-Ph$_3$C$_2$ as its maximum peak decomposition temperature decreased to 348 °C. Similar relation was observed for E_2
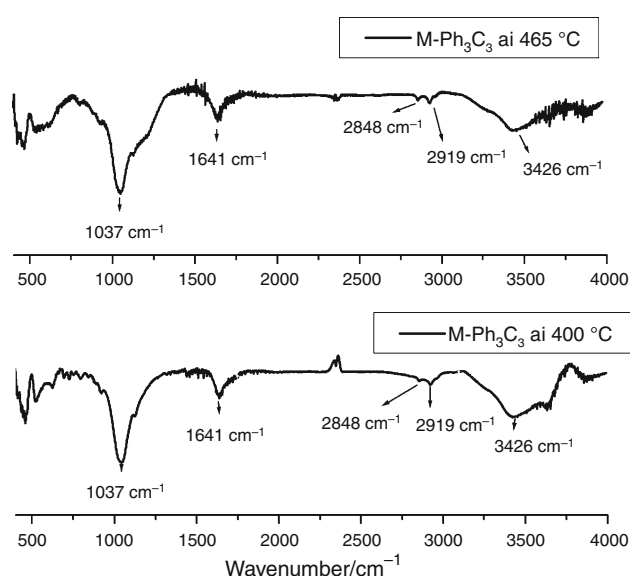
peak III with maximum peak decomposition temperature of peak III of the intercalated montmorillonites.

FTIR analysis

FTIR analysis of Ph$_3$C$_3$, heated at the maximum peak decomposition temperature of peak II and peak III, was done (Fig. 20). The plots showed peaks at 2,848 and 2,919 cm^{-1} with very little intensity. The bands were for asymmetric and symmetric stretching of CH$_2$ group, respectively [38]. As major part of intercalated organics was decomposed at those temperatures, the peaks were most possibly due to the presence of trace amount of fragmented alkyl groups.

Conclusions

(1) During the decomposition of alkyl triphenyl phosphonium intercalated montmorillonites, surface adsorbed organics were desorbed and decomposed during lower temperature mass loss in DTG. Intercalated organics were decomposed at higher temperature.

(2) Activation energies of decomposition pathways were evaluated. For lower temperatures, activation energies were correlated with desorption and decomposition process of different surface layers. Mainly two reaction pathways contributed to the activation energies deduced during heat treatment at peak II temperature zone. The first one was due to a nucleophilic attack followed by a rearrangement reaction, and the other involved the cleavage of sp^2-C bond. During decomposition of organics at peak III temperature regions, mainly above said reaction pathways along with some other fragmentation processes were followed.

(3) The higher activation energy (E_2) at higher temperature peaks (peak II and peak III) was found to be dependent on the maximum peak decomposition temperature of the respective peaks.

(4) The decomposition pattern of highest chain length intercalate, i.e., M-Ph$_3$C$_{12}$ showed a total loss of surface adsorbed and intercalated organics at lower temperatures (265–355 °C) thereby disclosing the fact that it has lower thermal stability than the other selected intercalates.

(5) Thermal degradation mechanism was mainly dependent on the heating temperature, cationic head group, and chain length of intercalates.

Fig. 20 FTIR plot of M-Ph$_3$C$_1$ at different temperature

References

1. Alexandre M, Dubois P. Polymer-layered silicate nanocomposites: preparation, properties and uses of a new class of materials. Mater Sci Eng R. 2000;28:1–63.
2. Zhu J, Morgan AB, Lamelas FJ, Wilkie CA. Fire properties of polystyrene-clay nanocomposites. Chem Mater. 2001;13:3774–80.
3. Sinha Ray S, Okamoto M. Polymer/layered nanocomposites: a review from preparation to processing. Prog Polym Sci. 2003;28:1539–641.
4. Ruiz-Hitzky E, Aranda P, Serratosa JM. Clay organic interactions: organoclay complexes and polymer–clay nanocomposites, Chap. 3. In: Auerbach S, Carrado KA, Dutta P, editors. Handbook of layered materials. New York: Marcel Dekker; 2004. p. 91–154.
5. Bergaya F, Theng BKG, Lagaly G. Handbook of clay science, developments in clay science, vol. 1. Amsterdam: Elsevier Ltd; 2006.
6. Patel HA, Somani RS, Bajaj HC, Jasra RV. Nanoclays for polymer nanocomposites, paints, inks, greases and cosmetics formulations, drug delivery vehicle and waste water treatment. Bull Mater Sci. 2006;29:133–45.
7. Maguy J, Lambert JF. A new nanocomposite: LDOPA/laponite. J Phys Chem Lett. 2010;1:85–8.
8. Grim Ralph E. Clay mineralogy. 2nd ed. New York: McGraw Hill; 1968.
9. Theng BKG. The chemistry of clay-organic reactions. New York: Wiley; 1974.
10. Emmerich K, Wolters F, Kahr G, Lagaly G. Clay profiling: the classification of montmorillonites. Clays Clay Miner. 2009;57:104–14.
11. Xie W, Gao Z, Pan WP, Hunter D, Singh A, Vaia R. Thermal degradation chemistry of alkyl quaternary ammonium montmorillonite. Chem Mater. 2001;13:2979–90.
12. Fajnor VS, Hlavaty V. Thermal stability of clay/organic intercalation complexes. J Therm Anal Calorim. 2002;67:113–8.
13. Xie W, Xie R, Pan WP, Hunter D, Koene B, Tan LS, et al. Thermal stability of quaternary phosphonium modified montmorillonites. Chem Mater. 2002;14:4837–45.
14. Xi Y, Zhou Q, Frost R, He H. Thermal stability of octadecyltrimethylammonium bromide modified montmorillonite organoclay. J Colloid Interface Sci. 2007;311:347–53.
15. Onal M, Sarikaya Y. Thermal analysis of some organoclays. J Therm Anal Calorim. 2008;91:261–5.
16. Ganguly S, Dana K, Ghatak S. Thermogravimetric study of n-alkylammonium-intercalated montmorillonites of different cation exchange capacity. J Therm Anal Calorim. 2010;100:71–8.
17. Avalos F, Ortiz JC, Zitzumbo R, Manchado MAL, Verdejo R, Arroyo M. Phosphonium salt intercalated montmorillonites. Appl Clay Sci. 2009;43:27–32.
18. Li Z, Jhang WT. Interlayer conformations of intercalated dodecyltrimethylammonium in rectorite as determined by FTIR, XRD, and TG analysis. Clays Clay Miner. 2009;57:194–204.
19. Yariv S, Ovadyahu D, Nasser A, Shuali U, Lahav N. Thermal analysis study of heat of dehydration of tributylammonium smectites. Thermochim Acta. 1992;207:103–13.
20. Balek V, Malek Z, Yariv S, Matuschek G. Characterization of montmorillonite saturated with various cations. J Therm Anal Calorim. 1999;56:67–76.
21. Yariv S. The role of charcoal on DTA curves of organo-clay complexes: an overview. Appl Clay Sci. 2004;24:225–36.
22. Abramova E, Lapides I, Yariv S. Thermo-XRD investigation of monoionic montmorillonites mechanochemically treated with urea. J Therm Anal Calorim. 2007;90:99–106.
23. Halim NA, Ibrahim ZA, Ahmad AB. Intercalation of water and guest molecules within Ca^{2+}—montmorillonite DSC studies in low temperature range. J Therm Anal Calorim. 2010;102(3):983–8.
24. Achilias DS, Nikolaidis AK, Karayannidis GP. PMMA/organo-modified montmorillonite nanocomposites prepared by in situ bulk polymerization, study of the reaction kinetics. J Therm Anal Calorim. 2010;102(2):451–60.
25. Bayram H, Muserref O, Hamza Y, Yiiksel S. Thermal analysis of a white calcium bentonite. J Therm Anal Calorim. 2010;101(3):873–9.
26. Leite FI, Priscilla S, Soares A, Carvalho LH, Rapso CMO, Matts ML. Characterization of pristine and purified organo-bentonites. J Therm Anal Calorim. 2010;100(2):563–9.
27. Lu L, Cai J, Frost RL. Desorption of stearic acid upon surfactant adsorbed montmorillonite, a thermogravimetric study. J Therm Anal Calorim. 2010;100(1):141–4.
28. Girgis BS, El-Barawy KA, Feli NS. Dehydration kinetics of some smectites: a thermogravimetric study. Thermochim Acta. 1986;98:181–9.
29. Guler C, Sarier N. Kinetics of thermal dehydration of acid-activated montmorillonite by the rising temperature technique. Thermochim Acta. 1990;159:29–33.
30. Murray P, White J. Kinetics of the thermal dehydration of clays. Trans Br Ceram Soc. 1949;48:187–206.
31. Murray P, White J. Kinetics of the thermal dehydration of clays. Part 1. Dehydration characteristics of the clay minerals. Trans Br Ceram Soc. 1955;54:137–49.
32. Murray P, White J. Kinetics of the thermal dehydration of clays. Part II. Isothermal decomposition of the clay minerals. Trans Br Ceram Soc. 1955;54:151–87.
33. Murray P, White J. Kinetics of the thermal dehydration of clays. Part III. Kinetics analysis of mixtures of the clay minerals. Trans Br Ceram Soc. 1955;54:189–203.
34. Murray P, White J. Kinetics of the thermal dehydration of clays. Part IV. Interpretation of the differential thermal analysis of the clay minerals. Trans Br Ceram Soc. 1955;54:204–38.
35. Bray HJ, Redfern SAT. Kinetics of dehydration of Ca-montmorillonite. Phys Chem Miner. 1999;26:591–600.
36. Mehlich A. Determination of cation- and anion-exchange properties of soils. Soil Sci. 1948;66:429–45.
37. Bache BW. The measurement of cation exchange capacity of soils. J Sci Food Agric. 1976;27:273–80.
38. Patel HA, Somani RS, Bajaj HC, Jasra RV. Preparation and characterization of phosphonium montmorillonite with enhanced thermal stability. Appl Clay Sci. 2007;35:194–200.